Tunable, Dielectric-Loaded Microwave Cavities Capable of High Q and High Filling Factor*

E. O. AMMANN†, STUDENT MEMBER, IEEE, AND R. J. MORRIS‡, MEMBER, IEEE

Summary—Many applications require the presence of a dielectric inside a microwave resonator. This paper presents a new type of dielectric-loaded cavity and contains a detailed analysis of its properties. The cavity consists of a waveguide of arbitrary but uniform cross section, filled with dielectric for part of its length, with movable shorting plungers in the guide beyond one or both ends of the dielectric. Such a structure supports resonances at frequencies where a particular waveguide mode is above cutoff in the dielectric, but below cutoff outside. These resonances can have high Q's, especially when the cavity ends are open. Frequency tuning is possible via the movable plungers.

The present analysis investigates resonant frequency, tuning range, and electric and magnetic filling factors. Wall losses are calculated for the particular case of a circular cross section. All results are plotted as universal design curves. The results indicate that this configuration is quite versatile and should be useful in numerous applications, including microwave solid-state masers, microwave light modulators, and the study of "ghost mode" resonances in waveguide windows.

I. Introduction

THIS PAPER summarizes a recent study [1] of a new class of tunable, dielectric-loaded microwave cavities. Two forms of cavity, shown in Fig. 1, are treated. In both forms, a piece of homogeneous, isotropic dielectric is placed in a uniform waveguide of arbitrary cross section with movable shorting plungers at one or both ends. The dielectric sample is machined so that: 1) its outer surface closely fits the waveguide walls, and 2) the two parallel faces of the dielectric are perpendicular to the waveguide axis. In the single-ended version, the waveguide is terminated by an electric short at one of the parallel faces of the dielectric.

Both cavity types support high-Q resonances at frequencies which are below the cutoff frequency of the unloaded waveguide, but above the cutoff frequency of the dielectric-loaded waveguide. Fields corresponding to these resonances have propagating character inside the dielectric (*i.e.*, oscillatory longitudinal variation), while decaying outside. If the unloaded section is many decay constants long, negligible fields exist at the shorting plunger (which can then be omitted), and a high-Q resonance is maintained. The transverse field configurations are identical to those of ordinary waveguide modes.

* Received May 24, 1963; revised manuscript received August 8, 1963. This work was supported by the Aeronautical Systems Division of the United States Air Force under Contract AF33(616)-7944; additional support was provided by the United States Army Signal Corps under Contract DA36-039 SC-85387.

† Sylvania Microwave Device Division, Mountain View, Calif. Formerly with Stanford Electronics Labs., Stanford University, Stanford, Calif.

‡ Stanford Electronics Labs., Stanford University, Stanford, Calif.

Frequency tuning is accomplished by moving the shorting plunger(s). When the unloaded waveguide is well below cutoff, the resonant fields are primarily confined to the dielectric. In such cases, relatively high unloaded Q's are obtained even if the plunger is of the noncontacting variety. It is usually best to separate the plunger from the waveguide wall by thin dielectric spacers in order to avoid contact losses and consequent erratic behavior of the Q with plunger motion. Since the fields in the propagating section are much larger than those in the cutoff sections, the coupling structure should be located near the dielectric (see Fig. 1).

Many advantages of these cavities are derived from the possibility of obtaining three features simultaneously in one design: 1) a major fraction of the electric or magnetic stored energy (or both) can be in the dielectric (*i.e.*, high filling factors); 2) the resonant frequency can be tuned over a large range, often an octave or more; and 3) the resonance can possess a high unloaded Q. This type of cavity can achieve all three features—if properly designed—without significantly compromising any of them.

The single-ended cavity was first used by Morris [2] in an X-band microwave maser. To the authors' knowledge, the tunable double-ended cavity has not been used elsewhere. The double-ended cavity with tuning plungers removed is identical to a dielectric waveguide window. Resonances in such a structure have been termed "ghost modes" by Jaynes [3] and have been analyzed by Jaynes and Forrer [4], [5]. Their analysis was motivated by the destructive effects these resonances have upon windows in high-power klystrons.

These cavities appear to be useful both as tunable and as fixed-frequency microwave resonators. They appear particularly attractive in the areas of solid-state microwave masers, paramagnetic resonance spectroscopy, microwave light modulators, microwave measurements, and as compact—yet tunable—microwave resonators. Furthermore, the information presented here has direct application to resonances in waveguide windows, and may be especially useful in the development of very high-power microwave tubes.

This paper contains a general analysis of the dielectric-loaded cavity for arbitrary waveguide cross sections. Transcendental equations are obtained, whose solutions (found on a digital computer) give the cavity resonant frequencies. Calculations are made of the cavity tuning range, and of the electric and magnetic filling factors. For the particular case of a circular cross sec-

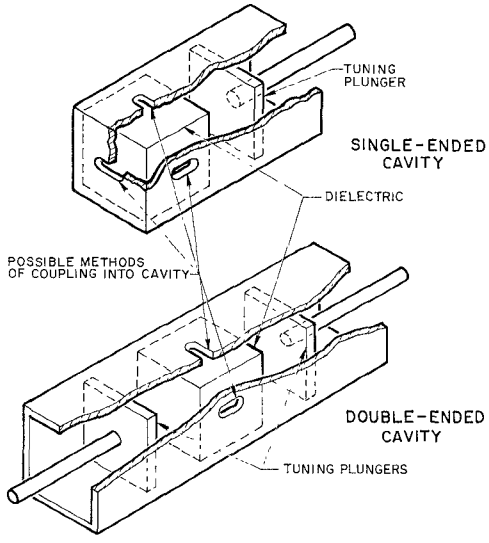

Fig. 1—Tunable, dielectric-loaded microwave cavities.

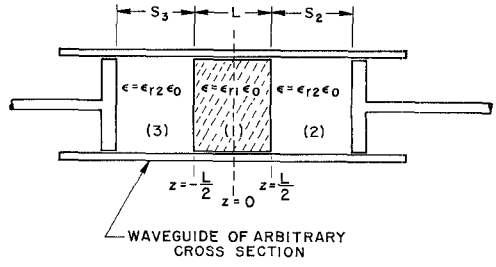

Fig. 2—Double-ended cavity configuration.

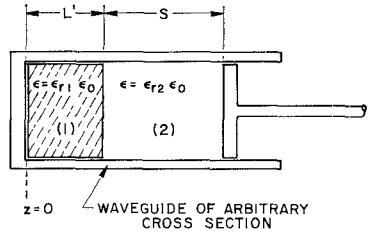

Fig. 3—Single-ended cavity configuration.

tion, unloaded Q due to wall losses is calculated for several low order modes. All data is presented in the form of graphs for easy use in cavity design. The information in this paper, plus considerable additional information, is available in a report [1] by the authors.

II. Derivation of General Cavity Equations

In this section we derive various quantities for the double- and single-ended cavities of Figs. 2 and 3. The analyses assume that the waveguide forming the cavity is a uniform, lossless cylinder of arbitrary cross section. All cavity regions are assumed to be filled with homogeneous, isotropic dielectric, the dielectrics in regions 2 and 3 being identical. The waveguide modes under consideration are assumed to be propagating in region 1 while being cut off in regions 2 and 3. The relative dielectric constant ϵ_{r2} of the cutoff regions is less than ϵ_{r1} of region 1, such that $\epsilon_{r1}/\epsilon_{r2}=K$, where $K>1$. Regions 2 and 3 will often contain only air, in which case $K=\epsilon_{r1}$.

A. Double-ended Cavity

Consider propagation of TE waves in the configuration of Fig. 2. In terms of transverse and longitudinal components of a particular waveguide mode, the general field quantities for a TE traveling wave are related by [6]

$$\boldsymbol{H}_t = \mp \frac{\gamma}{k_c^2} \nabla_t H_z \tag{1a}$$

$$\boldsymbol{E}_t = \mp \frac{j\omega\mu}{\gamma} (\boldsymbol{a}_z \times \boldsymbol{H}_t). \tag{1b}$$

The subscripts t and z denote transverse and longitudinal components respectively. $\boldsymbol{E}_t$ and $\boldsymbol{H}_t$ are two-dimensional vectors in the transverse plane, and the operator ∇_t is a transverse two-dimensional gradient. Other quantities are related thus:

$$k_c^2 = \gamma^2 + \epsilon_r k_0^2, \quad \text{where} \quad k_0^2 = \omega^2\mu_0\epsilon_0.$$

The parameter $k_c=2\pi/\lambda_c$, where λ_c is the cutoff wavelength for the particular waveguide mode; λ_c is determined only by the cross-sectional geometry and by the order of transverse mode variation. The propagation constant is $\gamma=\alpha+j\beta$, and all fields are assumed to vary with z as $\exp(j\omega t \mp \gamma z)$ so that the upper and lower signs in (1) are for forward and backward waves, respectively. In a lossless waveguide, γ is either purely real or purely imaginary, depending on whether the guide is below or above cutoff. For the three regions in Fig. 2, we have

Region 1:

$$\gamma = j\beta = j\sqrt{\epsilon_{r1}k_0^2 - k_c^2} \tag{2a}$$

Region 2 and 3:

$$\gamma = \alpha = \sqrt{k_c^2 - \epsilon_{r2}k_0^2}. \tag{2b}$$

For a single TE waveguide mode, H_z can be shown to have the following form,

Region 1:

$$H_z = T(x, y)[G \sin \beta z + H \cos \beta z] \tag{3a}$$

Region 2:

$$H_z = C_2 T(x, y) \sinh \alpha[z - (L/2 + S_2)] \tag{3b}$$

Region 3:

$$H_z = C_3 T(x, y) \sinh \alpha[z + (L/2 + S_3)]. \tag{3c}$$

The quantity $T(x, y)$ is a two-dimensional scalar function that gives the transverse dependence of H_z in terms of arbitrary transverse coordinates. $T(x, y)$ must satisfy the side-wall boundary conditions imposed by the cavity. The arbitrary constants G and H give a measure of the oddness and evenness of H_z with respect to the plane $z=0$ since they multiply the sin βz and cos βz terms of (3a). The expressions in (3) are legitimate solutions since they include forward and backward waves and are as arbitrary as possible, subject to the boundary conditions $H_z=0$ at $z=(L/2+S_2)$ and at $z=-(L/2+S_3)$.

From (1) we have

$$\boldsymbol{E}_t = \frac{j\omega\mu}{k_c^2}(\boldsymbol{a}_z \times \nabla_t H_z), \tag{4}$$

which means that by setting $H_z = 0$ at the conducting shorts, we also do the same for $\boldsymbol{E}_t$. Substituting forward- and backward-wave terms of (3) into (1a), we obtain for $\boldsymbol{H}_t$,

Region 1:

$$\boldsymbol{H}_t = \frac{\beta}{k_c^2}\nabla_t T(x, y)[G\cos\beta z - H\sin\beta z] \tag{5a}$$

Region 2:

$$\boldsymbol{H}_t = \frac{\alpha}{k_c^2}\nabla_t T(x, y)C_2\cosh\alpha[z - (L/2 + S_2)] \tag{5b}$$

Region 3:

$$\boldsymbol{H}_t = \frac{\alpha}{k_c^2}\nabla_t T(x, y)C_3\cosh\alpha\,[z + (L/2 + S_3)]. \tag{5c}$$

We must match field expressions at the dielectric interfaces, $z = \pm L/2$. Because of (4), it is sufficient to match H_z and $\boldsymbol{H}_t$, since matching H_z automatically matches $\boldsymbol{E}_t$. By matching H_z and $\boldsymbol{H}_t$ at $z = \pm L/2$, we can eliminate the arbitrary constants C_2 and C_3 to eventually obtain

$$G\left(\alpha\tan\frac{\beta L}{2} + \beta\tanh\alpha S_2\right) = H\left(\beta\tan\frac{\beta L}{2}\tanh\alpha S_2 - \alpha\right) \tag{6a}$$

$$G\left(\alpha\tan\frac{\beta L}{2} + \beta\tanh\alpha S_3\right) = -H\left(\beta\tan\frac{\beta L}{2}\tanh\alpha S_3 - \alpha\right). \tag{6b}$$

The general characteristic equation which determines the resonant value of ω for $S_2 \neq S_3$ is obtained by dividing (6a) by (6b).

For the case of equal plunger positions ($S_2 = S_3 = S$), (6) is in the form

$$Gf(\omega) = Hg(\omega)$$
$$Gf(\omega) = -Hg(\omega).$$

Here the cavity resonant frequency ω (contained in α and β), is the unknown; it must have a value such that (6) is satisfied. The only consistent solutions are

$$G = 0, \qquad g(\omega) = 0,$$

$$\text{TE EVEN modes: } \beta\tan\frac{\beta L}{2} = \alpha\coth\alpha S, \tag{7a}$$

and

$$H = 0, \qquad f(\omega) = 0,$$

$$\text{TE ODD modes: } \alpha\tan\frac{\beta L}{2} = -\beta\tanh\alpha S. \tag{7b}$$

The designations EVEN and ODD refer to the symmetry of H_z with respect to the plane $z = 0$.

For the case of TM waves, a similar analysis leads to expressions comparable to (6)

$$G'\left(\beta + \alpha K\tan\frac{\beta L}{2}\tanh\alpha S_2\right) = H'\left(\beta\tan\frac{\beta L}{2} - \alpha K\tanh\alpha S_2\right) \tag{8a}$$

$$G'\left(\beta + \alpha K\tan\frac{\beta L}{2}\tanh\alpha S_3\right) = -H'\left(\beta\tan\frac{\beta L}{2} - \alpha K\tanh\alpha S_3\right). \tag{8b}$$

The general TM characteristic equation which determines ω is obtained by dividing (8a) by (8b). When $S_2 = S_3 = S$, (8) gives the following characteristic equations:

$$\text{TM EVEN modes: } \beta\tan\frac{\beta L}{2} = K\alpha\tanh\alpha S \tag{9a}$$

$$\text{TM ODD modes: } K\alpha\tan\frac{\beta L}{2} = -\beta\coth\alpha S. \tag{9b}$$

When both plungers are removed, $S = \infty$, and, consequently, $\tanh\alpha S = \coth\alpha S = 1$. Then the TE and TM characteristic equations are (7) and (9) with $\tanh\alpha S$ and $\coth\alpha S$ replaced by unity.

B. Single-ended Cavity

The single-ended cavity (Fig. 3) is a special case of the double-ended cavity, being obtained from it by inserting a conducting plane at $z = 0$. An analysis similar to that just outlined could be performed to obtain characteristic equations for the single-ended cavity. This can be avoided, however, if we notice that the double-ended cavity fields corresponding to TE ODD and TM EVEN modes also satisfy the boundary conditions for a single-ended cavity. Thus we may use these double-ended cavity results for the single-ended cavity by replacing $L/2$ by L'.

The characteristic equations for the single-ended cavity are

$$\text{TE Waves: } \alpha\tan\beta L' = -\beta\tanh\alpha S \tag{10a}$$

$$\text{TM Waves: } \beta\tan\beta L' = K\alpha\tanh\alpha S. \tag{10b}$$

For the plunger removed, $S=\infty$, and the characteristic equations are (10) with $\tanh \alpha S$ replaced by unity. In all of the characteristic equations, the unknown quantity is the cavity resonant frequency ω which satisfies the equations for particular values of the parameters K, k_c, S, and L (or L'). The exact solutions for ω, which are later presented in graphical form, were obtained on a digital computer. However, the approximate behavior of the solution can readily be seen from the graphical method presented in Fig. 4. This figure illustrates solution of the single-ended cavity characteristic equation for both TE and TM waves. We have drawn plots of the left- and right-hand sides of (10). The resonant frequencies are given by the intersections of the two curves. The right-hand side of (10) is shown as a family of curves corresponding to different values of the plunger position S; the left-hand side is a somewhat modified tangent function. It can be seen that as the plunger position is moved from $S=0$ to a very large value, *the resonant frequency of a TE mode tunes down, whereas the resonant frequency of a TM mode tunes up*. The condition $S=0$ corresponds to the conventional propagating, dielectric-filled cavity. The first branch in the TM case corresponds, if we take $S=0$, to conventional TM_{uv0} modes, the second branch to TM_{uv1} modes, etc. The lowest frequency solution in the TE case corresponds to TE_{uv1} modes. Note that since TE modes tune down in frequency and TM modes tune up as S is increased, there is the possibility of a given TE mode being crossed as it tunes down by TM modes which are tuning up. The double-ended characteristic equations can be shown to give tuning in a similar manner.

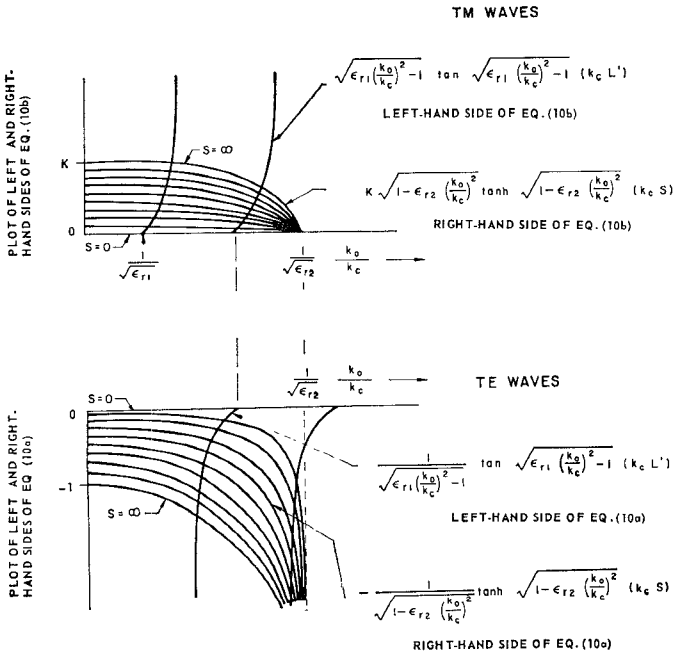

Fig. 4—Graphical technique for solving the characteristic equations (10) of the single-ended cavity.

C. Dielectric Losses

We here consider dielectric losses in a cavity of arbitrary cross section, and account for them by a quantity Q_{DL},

$$Q_{DL} = \frac{\omega(\text{Total Energy Stored in Cavity})}{(\text{Total Power Dissipated in all Dielectrics})}. \quad (11)$$

Consider the configuration of Fig. 2 with both plungers removed, and assume that region 1 is filled with a dielectric of permittivity $\epsilon_{r1}\epsilon_0$ and uniform conductivity σ_1, while regions 2 and 3 are both filled with a material described by $\epsilon_{r2}\epsilon_0$ and σ_2. The following can then be shown:

$$\frac{1}{Q_{DL}} = \frac{\dfrac{\sigma_1}{\omega\epsilon_{r1}\epsilon_0} U_1 + \dfrac{\sigma_2}{\omega\epsilon_{r2}\epsilon_0}(U_2 + U_3)}{U_T},$$

where U_1, U_2, and U_3 are the electric energies stored in regions 1, 2, and 3, and $U_T = U_1 + U_2 + U_3$. We recognize $\sigma_1/\omega\epsilon_{r1}\epsilon_0$ and $\sigma_2/\omega\epsilon_{r2}\epsilon_0$ as being the loss tangents, $\tan \delta_1$ and $\tan \delta_2$, of the two dielectric materials. We therefore have

$$\frac{1}{Q_{DL}} = (\tan \delta_1)\frac{U_1}{U_T} + (\tan \delta_2)\left(1 - \frac{U_1}{U_T}\right). \quad (12)$$

The ratio U_1/U_T is the ratio of electric energy in region 1 to the total electric energy. Plots for this ratio are given in Fig. 7.

III. Circular Cross-Sectional Cavities

A case of considerable interest is a cavity with circular cross section. In their report [1], the authors have presented complete expressions for the fields in double- and single-ended circular cavities with plungers removed. Also presented there are expressions for the unloaded Q due to wall losses, which are given below.

A. Wall Losses

The unloaded Q due to losses in the cavity walls—denoted by Q_{WL} here—was calculated for double- and single-ended cavities of circular cross section, assuming that the plungers were removed. The results of this section can be used in conjunction with those for dielectric losses, of Section II-C, to obtain an exact value for the net unloaded Q,

$$1/Q = 1/Q_{WL} + 1/Q_{DL}. \quad (13)$$

The definition of Q_{WL} is

$$Q_{WL} = \frac{\omega_0(\text{Total Energy Stored in Cavity})}{\text{Total Power Dissipated in Cavity Walls}}. \quad (14)$$

Using the field equations presented in the report [1], the total stored energy and dissipated power were found by performing appropriate integrations over the cavity volume and surfaces. A normalized form [7] of Q_{WL}

was used, namely $Q_{WL}\delta/\lambda_1$. The δ refers to skin depth, while λ_1 is wavelength in the dielectric of region 1.

For the double-ended cavity, stored energy is present in regions 1, 2, and 3, while power is dissipated in the sidewalls of the same regions. Because both plungers are removed, there are no end-wall losses. The expressions for $Q_{WL}\delta/\lambda_1$ were found to be:

a) TE EVEN modes (TE_{lm1}, TE_{lm3}, TE_{lm5}, $\cdots$)

$$\frac{Q_{WL}\delta}{\lambda_1} = \frac{(r_{lm}'^2 - l^2)\left(\sqrt{\epsilon_{r1}}\frac{k_0}{k_c}\right)^3\left\{K\left[k_cL + \frac{k_c}{\beta}\sin\beta L\right] + \left[\frac{k_c}{\alpha}(1+\cos\beta L)\right]\right\}}{2\pi r_{lm}'K\left\{\left[k_cL + \frac{k_c}{\beta}\sin\beta L\right] + \left(\frac{l}{r_{lm}'}\right)^2\left(\frac{\beta}{k_c}\right)^2\left(k_cL - \frac{k_c}{\beta}\sin\beta L\right) + \left[\frac{k_c}{\alpha}(1+\cos\beta L)\right]\left[1+\left(\frac{l}{r_{lm}'}\right)^2\left(\frac{\alpha}{k_c}\right)^2\right]\right.} \tag{15}$$

b) TE ODD modes (TE_{lm2}, TE_{lm4}, TE_{lm6}, $\cdots$)

$$\frac{Q_{WL}\delta}{\lambda_1} = \frac{(r_{lm}'^2 - l^2)\left(\sqrt{\epsilon_{r1}}\frac{k_0}{k_c}\right)^3\left\{K\left[k_cL - \frac{k_c}{\beta}\sin\beta L\right] + \left[\frac{k_c}{\alpha}(1-\cos\beta L)\right]\right\}}{2\pi r_{lm}'K\left\{\left[k_cL - \frac{k_c}{\beta}\sin\beta L\right] + \left(\frac{l}{r_{lm}'}\right)^2\left(\frac{\beta}{k_c}\right)^2\left(k_cL + \frac{k_c}{\beta}\sin\beta L\right) + \left[\frac{k_c}{\alpha}(1-\cos\beta L)\right]\left[1+\left(\frac{l}{r_{lm}'}\right)^2\left(\frac{\alpha}{k_c}\right)^2\right]\right\}} \tag{16}$$

c) TM EVEN modes (TM_{lm0}, TM_{lm2}, TM_{lm4}, $\cdots$) and TM ODD modes (TM_{lm1}, TM_{lm3}, TM_{lm5}, $\cdots$)

$$\frac{Q_{WL}\delta}{\lambda_1} = \frac{r_{lm}}{2\pi}\left(\sqrt{\epsilon_{r1}}\frac{k_0}{k_c}\right). \tag{17}$$

For the single-ended cavity, energy is stored in regions 1 and 2. Power dissipation occurs in the sidewalls of regions 1 and 2, and in addition, in the end wall which bounds region 1. For this reason, unlike other quantities previously discussed, $Q_{WL}\delta/\lambda_1$ expressions for the single-ended cavity are not derivable from the double-ended cavity results. Separate expressions were derived and are giveu below. As before, it is assumed that the tuning plunger is removed.

a) TE modes

$$\frac{Q_{WL}\delta}{\lambda_1} = \frac{(r_{lm}'^2 - l^2)\left(\sqrt{\epsilon_{r1}}\frac{k_0}{k_c}\right)^3\left\{K\left[2k_cL' - \frac{k_c}{\beta}\sin 2\beta L'\right] + \left[\frac{k_c}{\alpha}(1-\cos 2\beta L')\right]\right\}}{2\pi r_{lm}'K\left\{\left[2k_cL' - \frac{k_c}{\beta}\sin 2\beta L'\right] + \left(\frac{l}{r_{lm}'}\right)^2\left(\frac{\beta}{k_c}\right)^2\left[2k_cL' + \frac{k_c}{\beta}\sin 2\beta L'\right]\right.} \tag{18}$$

$$\left. + \left[\frac{k_c}{\alpha}(1-\cos 2\beta L')\right]\left[1+\left(\frac{l}{r_{lm}'}\right)^2\left(\frac{\alpha}{k_c}\right)^2\right] + 2r_{lm}'\left(\frac{\beta}{k_c}\right)^2\left(1 - \frac{l^2}{r_{lm}'^2}\right)\right\}$$

b) TM modes

$$\frac{Q_{WL}\delta}{\lambda_1} = \frac{r_{lm}}{2\pi}\left(\sqrt{\epsilon_{r1}}\frac{k_0}{k_c}\right)\frac{\left[2k_cL' + \frac{k_c}{\beta}\sin 2\beta L' + \frac{k_c}{\alpha}(1+\cos 2\beta L')\right]}{\left[2k_cL' + \frac{k_c}{\beta}\sin 2\beta L' + \frac{k_c}{\alpha}(1+\cos 2\beta L') + 2r_{lm}\right]}. \tag{19}$$

In the above equations, r_{lm} is the mth zero of $J_l(x)$, and r_{lm}' is the mth zero of $J_l'(x)$. In the following section, graphs are plotted showing $Q_{WL}\delta/\lambda_1$ as a function of the diameter to length ratio, D/L, for the double-ended cavity, and as a function of D/L' for the single-ended cavity.

TABLE I

EQUIVALENCE BETWEEN GRAPH LABELS AND CAVITY MODES

Graph Label	Corresponding Mode in Double-Ended Cavity	Corresponding Mode in Single-Ended Cavity
TE EVEN, branch 1	TE_{uv1}	—
TM EVEN, branch 1	TM_{uv0}	TM_{uv0}
TE ODD, branch 1	TE_{uv2}	TE_{uv1}
TM ODD, branch 1	TM_{uv1}	—
TE EVEN, branch 2	TE_{uv3}	—
TM EVEN, branch 2	TM_{uv2}	TM_{uv1}
TE ODD, branch 2	TE_{uv4}	TE_{uv2}
TM ODD, branch 2	TM_{uv3}	—

TABLE II

INSTRUCTIONS FOR USING GRAPHS TO DETERMINE PROPERTIES OF SINGLE-ENDED AND DOUBLE-ENDED CAVITIES

Figure Numbers	Use of the Graph for	
	Double-Ended Cavity	Single-Ended Cavity
5(a), 5(d), 5(e), 5(h), 6(a), 6(d), 6(e), 6(h), 7(a), 7(d), 7(e), 7(h), 8(a), 8(d), 8(e), 8(h), 9(b), 9(d), 9(f), 9(h), 10(a), 10(b)	Use directly	—
5(b), 5(c), 5(f), 5(g), 6(b), 6(c), 6(f), 6(g), 7(b), 7(c), 7(f), 7(g), 8(b), 8(c), 8(f), 8(g)	Use directly	Change label of abscissa to $1/2k_cL'$
9(a), 9(c), 9(e), 9(g)	———	Use directly
10(c), 10(d)	Use directly	Change label of abscissa to $D/2L'$

IV. INTERPRETATION AND DISCUSSION OF GRAPHS

Much of the cavity information is contained in the graphs presented in this section. These graphs are solutions to and plots of the equations presented earlier; they show the following quantities:

1) plunger-out resonant frequency vs $1/k_cL$
2) cavity tuning range vs $1/k_cL$
3) electric filling factor vs $1/k_cL$
4) magnetic filling factor vs $1/k_cL$
5) $Q_{WL}\delta/\lambda_1$ vs D/L
6) cavity tuning range vs D/L.

The graphs which were plotted vs $1/k_cL$ apply to a cavity of arbitrary cross section, while the graphs plotted vs D/L are for a cavity of circular cross section. Each graph contains several curves, with each curve corresponding to a different value of the parameter K.

So that a great variety of data could be presented in the space available, the graphs are shown on a small scale. However, in the authors' report [1], the graphs presented here, and others as well, are displayed in a scale large enough that data can be read from them with two- and three-figure accuracy.

A. Use of the Graphs

As seen in Section II, equations for the single-ended cavity are easily obtained from double-ended equations. Correspondingly, one set of graphs suffices for both the single- and double-ended cases. The sole exception to this is in the calculation and plotting of $Q_{WL}\delta/\lambda_1$, where separate results are obtained for the two cases.

We now state how the graphs may be used for single- and double-ended cavitities. The equivalence between the graph label and the corresponding mode in a single- or double-ended cavity is shown in Table I.

Table II states how the graphs may be used either for single- or double-ended cavities.

B. Discussion of Graphical Results

1) *Plunger-Out Resonant Frequency:* Fig. 5 contains graphs showing normalized plunger-out resonant frequency vs $1/k_cL$. We note the following: for small values of $1/k_cL$, the value of $\sqrt{\epsilon_{r2}}k_0(\infty)^1/k_c$ is $1/\sqrt{K}$. As $1/k_cL$ is increased, the value of $\sqrt{\epsilon_{r2}}k_0(\infty)/k_c$ increases monotonically, finally reaching a value of unity for a sufficiently large $1/k_cL$. This value of $1/k_cL$ for which $\sqrt{\epsilon_{r2}}k_0(\infty)/k_c=1$ is the point where regions 2 and 3 start to propagate. It is called the critical value here, and depends upon the particular resonant mode in question. The critical value of $1/k_cL$ is easily found from the plunger-out characteristic equations, and is listed in Table III for various modes.

For values of $1/k_cL$ greater than the critical value, regions 2 and 3 will be propagating instead of cut off, and the determinantal equations are no longer applicable. The graphs presented in this paper show results only for values of $1/k_cL$ which are less than the critical value, since the situation of interest here occurs only when regions 2 and 3 are cut off.

[1] $k_0(\infty)$ is shorthand notation for $k_0(S_2=S_3=\infty)$. Similarly, $k_0(0)$ is shorthand notation for $k_0(S_2=S_3=0)$.

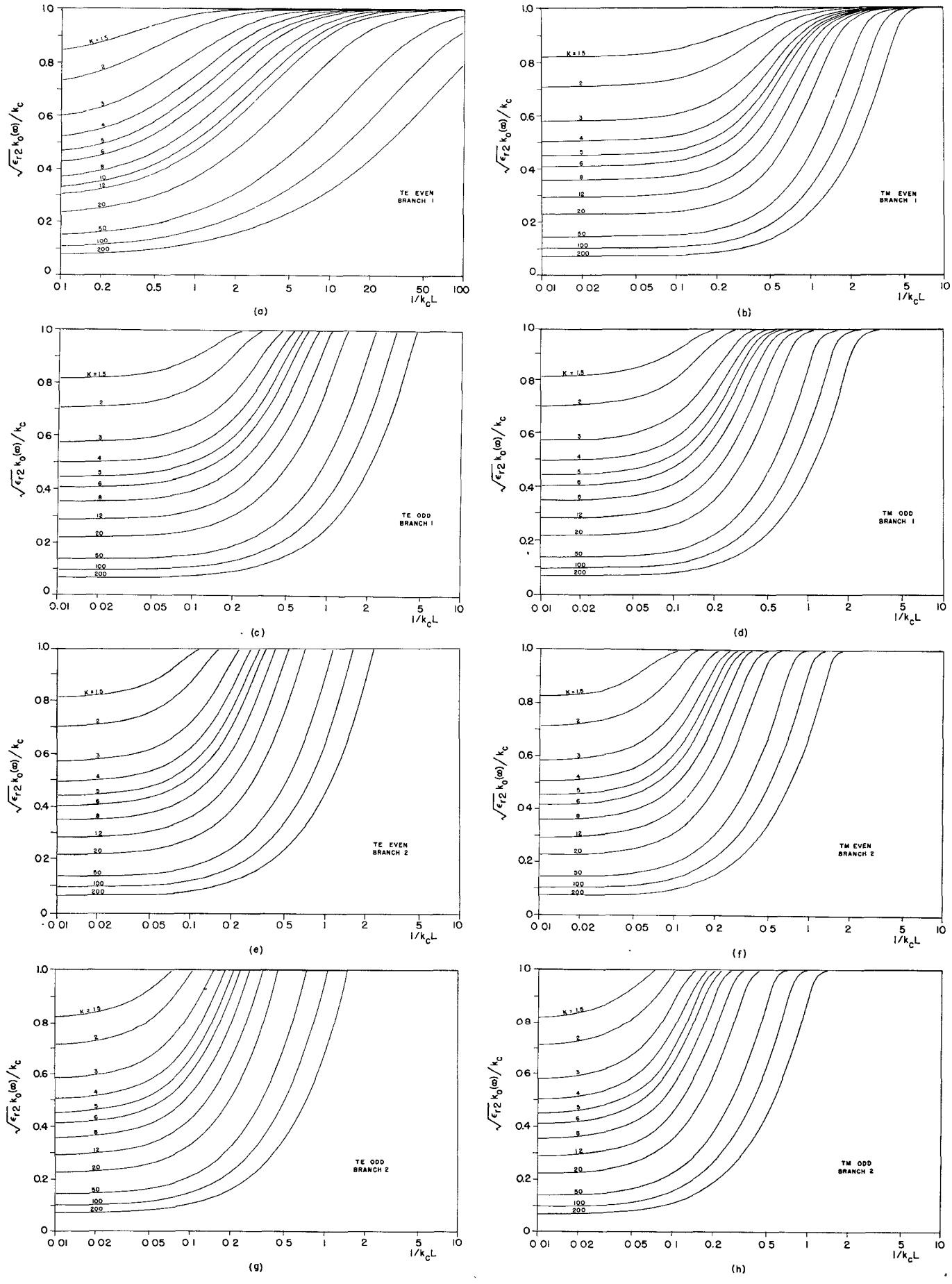

Fig. 5—Universal curves for cavity resonant frequency with plungers removed.

TABLE III
VALUES OF $1/k_cL$ AT WHICH REGIONS 2 AND 3 BECOME PROPAGATING

Critical Value of $1/k_cL$	Mode
∞	TE EVEN, branch 1
∞	TM EVEN, branch 1
$\sqrt{K-1}/\pi$	TE ODD, branch 1
$\sqrt{K-1}/\pi$	TM ODD, branch 1
$\sqrt{K-1}/2\pi$	TE EVEN, branch 2
$\sqrt{K-1}/2\pi$	TM EVEN, branch 2
$\sqrt{K-1}/3\pi$	TE ODD, branch 2
$\sqrt{K-1}/3\pi$	TM ODD, branch 2

2) *Cavity Tuning Range:* The graphs of Fig. 6 show the tuning range which is obtained when plungers are moved from completely in to completely out. For TE modes, $[k_0(0)-k_0(\infty)]/k_0(0)$ is plotted vs $1/k_cL$, while for TM modes, $[k_0(\infty)-k_0(0)]/k_0(0)$ is plotted vs $1/k_cL$.

Several interesting results can be seen from Fig. 6. For all TE modes, the tuning range increases with increasing $1/k_cL$, reaching its maximum value at the critical value. This maximum possible value of $[k_0(0)-k_0(\infty)]/k_0(0)$ is shown in Table IV.

For TM modes, the situation is considerably different. The per cent tuning range increases monotonically with increasing $1/k_cL$ for TM EVEN, branch 1 modes, but for all other TM modes, it peaks at some value of $1/k_cL$ which is less than the critical value, and then falls to zero at the critical value. The maximum possible value of $[k_0(\infty)-k_0(0)]/k_0(0)$ for TM EVEN branch 1 modes is $(\sqrt{K}-1)$. The maximum value for other TM modes is very difficult to calculate and was not found.

Finally we note that, for a given value of $1/k_cL$, the tuning range of TE modes *decreases* while the tuning range of TM modes *increases* as K is increased.

3) *Fraction of Magnetic and Electric Stored Energy in Region 1:* Figs. 7 and 8 (pp. 538–539) show, respectively, the fraction of the total stored electric and magnetic energies contained in region 1. These values were calculated by obtaining general field expressions for a cavity of arbitrary cross section and calculating stored energy in the various regions. The applicable equations are given in [1].

From Figs. 7 and 8 it is seen that is $1/k_cL$ increases, the electric and magnetic energies stored in region 1 decrease. This result we expect, for as $1/k_cL$ is increased, regions 2 and 3 are less strongly cut off, allowing the cavity fields to extend farther into these regions.

An interesting effect concerning the electric and magnetic stored energies should be noted. For a given $1/k_cL$ and K, the stored electric energy in region 1 will not equal the stored magnetic energy in region 1. This effect is explainable in the following manner. The *total* stored magnetic and electric energies in the cavity must, of course, be equal at resonance. But in each of the cutoff regions the stored electric and magnetic energies are not equal because a waveguide, which is below cutoff, has unequal electric and magnetic stored energies [8]. As a result, the electric and magnetic stored energies in region 1 are also unequal, the inequality being most pronounced when regions 2 and 3 are far below cutoff. For TE modes, there is more electric than magnetic stored energy in region 1, while the reverse is true for TM modes.

4) *Q_{WL} of Circular-Cylindrical Cavity:* The graphs of Fig. 9 show $Q_{WL}\delta/\lambda_1$ plotted as a function of D/L (and D/L') for cavities of circular cross section. These graphs are plots of (15)–(19). Also plotted on each graph is a curve labeled "conventional cavity" which shows $Q_{WL}\delta/\lambda_1$ for the dielectric-filled cavity formed by entirely enclosing region 1 with conducting surfaces. For TM modes in both the single- and double-ended cases, it can be shown that $Q_{WL}\delta/\lambda_1$ begins at a value of $r_{lm}/2\pi$ at $D/L=0$, and reaches a value of $r_{lm}\sqrt{K}/2\pi$ at the critical value of D/L. For TE modes, $Q_{WL}\delta/\lambda_1$ goes from a value of $(r_{lm}'^2-l^2)/2\pi r_{lm}'$ at $D/L=0$ to a value of $(r_{lm}'^2-l^2)\sqrt{K}/2\pi r_{lm}'$ at the critical value of D/L.

5) *Tuning Range of Circular Cylindrical Cavity:* The graphs of Fig. 10 show cavity tuning range as a function of D/L for various resonant modes in a cavity of circular cross section. These graphs are similar to those of Fig. 6, except that the abscissa $1/k_cL$ has been converted to D/L, and each graph corresponds to a particular mode.

V. ADVANTAGES AND USES OF THESE CAVITIES

The cavity designs described here are of potential interest in many situations which require a dielectric-loaded microwave cavity. We shall discuss some of the advantages of these cavities over more conventional designs, and include several possible applications.

A. Advantages

1) *Frequency Tunability while Maintaining a Large Filling Factor:* It is often desirable to completely (or nearly) fill a cavity with dielectric material. The designs of this paper provide a method of "filling" a cavity with dielectric, and yet allowing its frequency to be tuned.

We define *magnetic filling factor* here as the ratio of the magnetic stored energy in region 1 to the total magnetic stored energy in the cavity, and *electric filling factor* as the ratio of the electric stored energy in region 1 to the total electric stored energy. The electric and magnetic filling factors will vary as the cavity frequency is tuned, having their maximum values of unity when both tuning plungers are all the way in, and having their minimum values (given by Figs. 7 and 8) when both

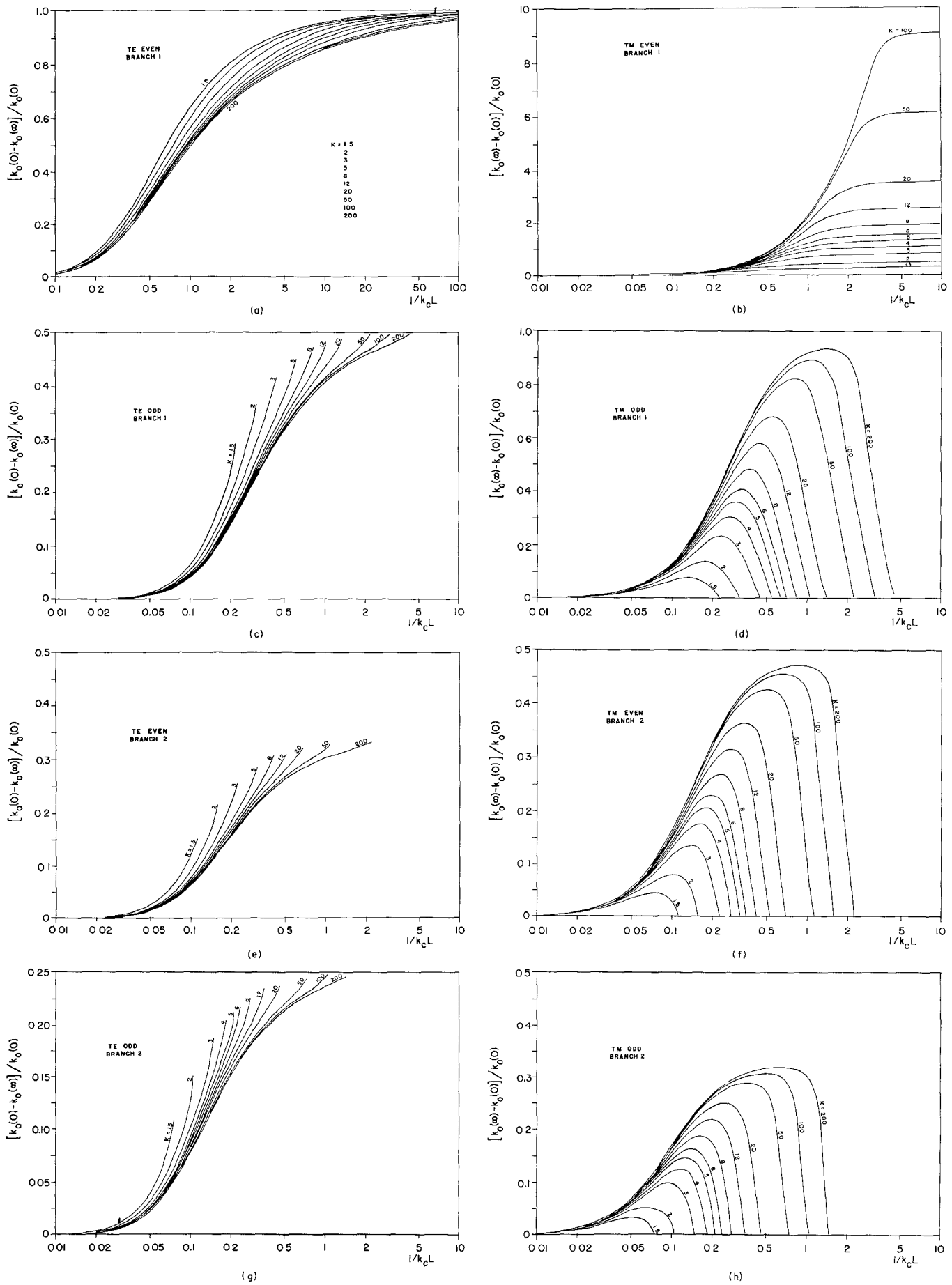

Fig. 6—Universal curves for cavity tuning range.

TABLE IV
MAXIMUM POSSIBLE VALUE OF TUNING RANGE FOR TE MODES

Maximum possible value of $[k_0(0) - k_0(\infty)]/k_0(0)$	Mode
1	TE EVEN, branch 1
$1 - \sqrt{\frac{K}{4K-3}}$	TE ODD, branch 1
$1 - 2\sqrt{\frac{K}{9K-5}}$	TE EVEN, branch 2
$1 - 3\sqrt{\frac{K}{16K-7}}$	TE ODD, branch 2

plungers are removed. If a large filling factor is wanted, its minimum value should be kept as large as possible.

The following results are noted from Figs. 6, 7, 8, and 10. If a cavity is designed for a small tuning range (*e.g.* 1 to 5 per cent), both the magnetic and electric filling factors will remain large (approximately 0.90 or more) throughout this range. If a cavity is designed for a moderate or large tuning range, it is often possible to keep one of the two filling factors large throughout the range. As explained in Section IV, the magnetic and electric filling factors will not, in general, be equal. A TE mode has a larger electric than magnetic filling factor, while the reverse is true of a TM mode. This should be an important consideration in choosing a cavity mode.

2) *Large Frequency Tuning with Moderate Plunger Displacements:* It is occasionally desirable to have a microwave cavity which is tunable over large (octave or more) frequency ranges. Large tuning ranges are possible using several conventional cavity designs, but these designs are often limited in their usefulness due to the large plunger displacements required. The designs of this paper offer a method of obtaining large frequency tuning ranges with moderate plunger displacements. Largest tuning ranges are obtained by using TE EVEN, branch 1, or TM EVEN, branch 1 modes, and by choosing a large value of $1/k_cL(\geq 1)$. The length of plunger motion required will depend upon the value of α, the plunger-out propagation constant, which is given by (2b). Plunger displacements of $5/\alpha$ for each of the tuning plungers should be adequate for complete tuning, since at this distance the cavity fields have fallen off to $(1/e)^5$ of their value at the dielectric boundary.

3) *TE and TM Modes Tune in Opposite Directions:* One of the interesting results concerning the cavities of this paper is that TE and TM modes tune in opposite directions. As a plunger is pulled out, TE modes tune down in frequency while TM modes tune up. This property is useful in several ways.

It can be used as an aid in identifying resonant modes. The direction that a mode tunes can be used to determine whether it is TE or TM, and the amount that it tunes (used in connection with Figs. 6 or 10) can be used to determine k_c. The reader should be cautioned that there may also be modes present which are propagating in regions 2 and 3 as well as in region 1; these modes will tune down in frequency when a plunger is pulled out, but will not approach a limiting frequency as the plungers are removed to infinity. A second method of determining the identity of a mode is to trace its field pattern within the cavity. By removing the plungers, one has complete access to the fields in regions 2 and 3. Using standard techniques [9], one can insert perturbing objects into these regions and determine the strength and direction of the field components.

The tuning properties of TE and TM modes are also useful for separating the TE_{011} and TM_{111} modes in a circular-cylindrical cavity. In a conventional circular cavity, as well as a double-ended circular cavity with both plungers pushed entirely in, the TE_{011} and TM_{111} resonant frequencies are degenerate. If one wishes to use the TE_{011} mode, some means must be provided for their separation. This separation is obtained by pulling out the plungers of the double-ended cavity, for the TM_{111} mode tunes up while the TE_{011} mode tunes down. If one needs only a fixed-tuned cavity, the plungers can be pulled out far enough to provide adequate separation of the two modes and then locked in position.

4) *Relatively Low Cavity Losses:* The cavities described here appear to be capable of quite good unloaded Q's. The two sources of loss are dielectric losses and wall losses. Using these cavities, the designer has control over the electric filling factor (see Fig. 7), and therefore has control over the dielectric losses. Wall losses are shown by the graphs of Fig. 9, where the solid curves give the plunger-out value of $Q_{WL}\delta/\lambda_1$ while the dotted curves (labeled conventional cavity) give the plunger-in value of $Q_{WL}\delta/\lambda_1$. For plunger positions between these two extremes, $Q_{WL}\delta/\lambda_1$ will fall somewhere between the two curves. Notice that in all cases except for TE_{111} modes, the double- and single-ended cavities have a higher $Q_{WL}\delta/\lambda_1$ than a conventional dielectric-filled cavity. This is because the cavity fields have decayed somewhat before they reach an end wall, resulting in reduced end wall losses.

5) *Double-ended Cavity Allows Simultaneous Control over* TWO *Resonant Frequencies:* One of the advantages of the double-ended cavity is that by the use of its two

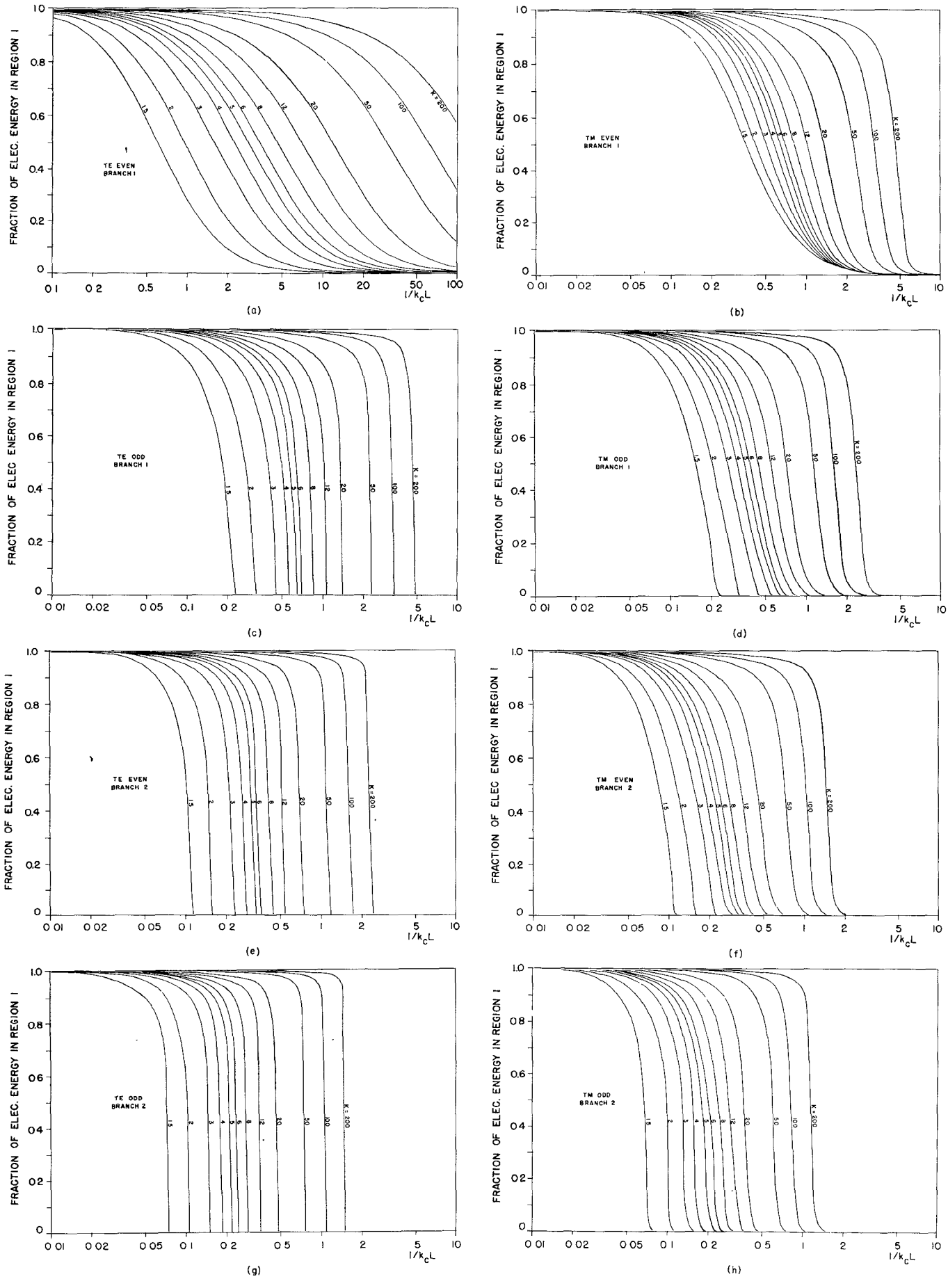

Fig. 7—Universal curves showing region 1 electrical energy divided by total electric energy.

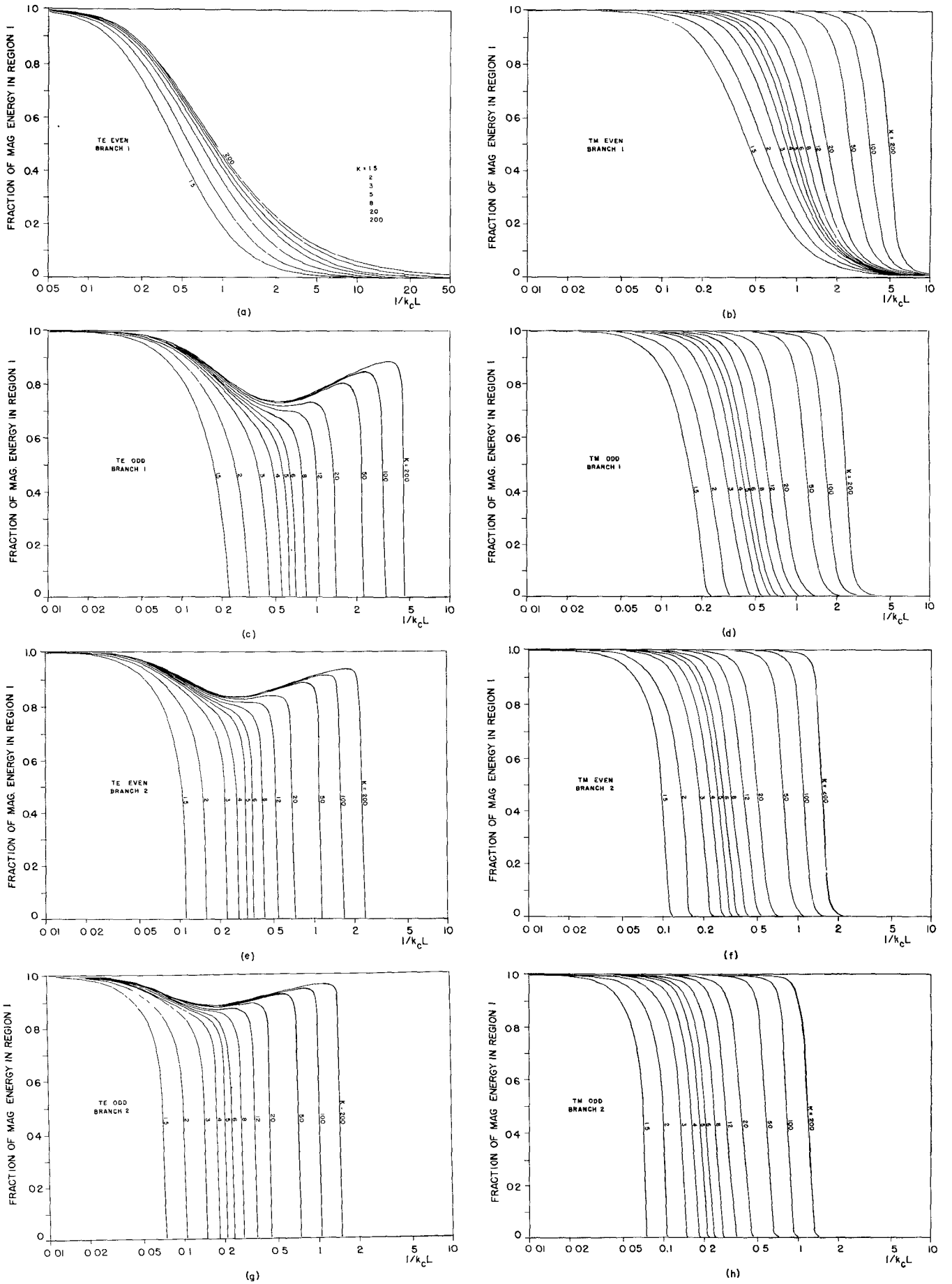

Fig. 8—Universal curves showing region 1 magnetic energy divided by total magnetic energy.

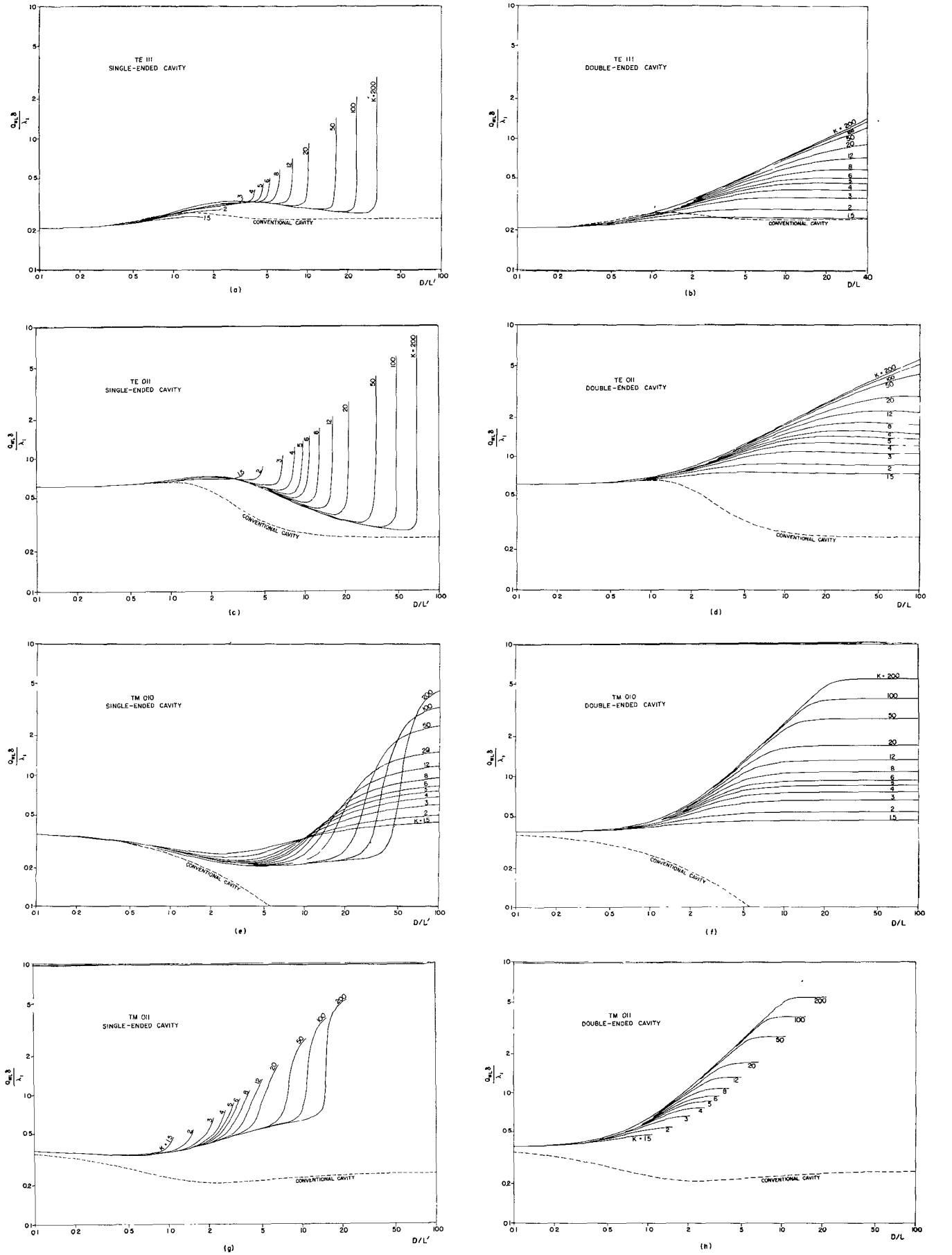

Fig. 9—Q of circular cylindrical cavity due to wall losses.

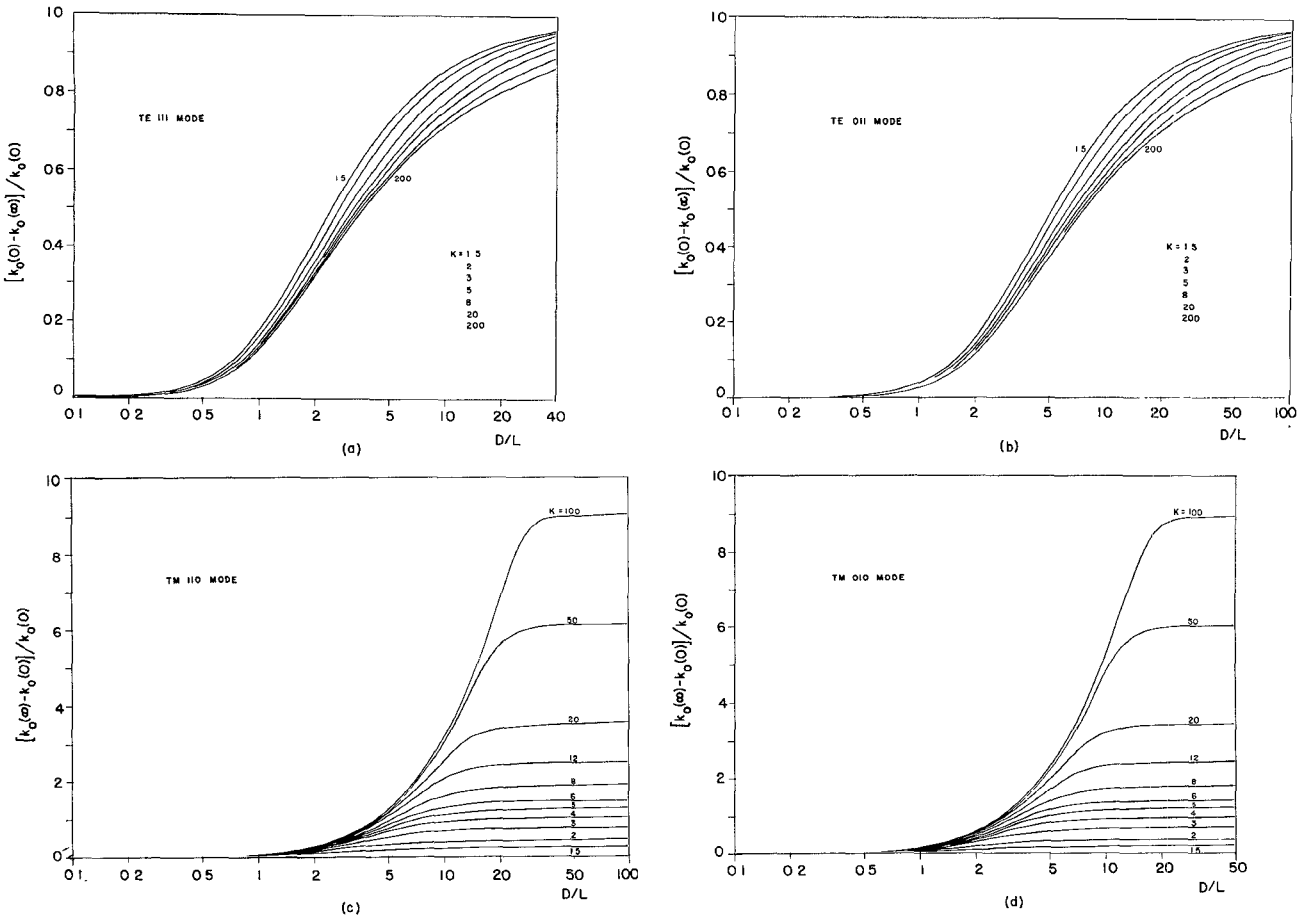

Fig. 10—Tuning range for circular cylindrical cavity.

plungers, one can control the frequencies of two resonant modes. In a cavity tuned by one plunger, which includes the single-ended cavity of this paper, one has frequency control over only one cavity mode at a time. If resonant mode A is tuned to a certain frequency f_A, we cannot in general separately tune another mode B to some f_B. In the double-ended cavity however, the additional plunger gives one an extra degree of freedom, enabling one to control mode A and mode B independently of one another. Of course, this does not mean that one plunger tunes mode A while the other plunger tunes mode B; rather, it means that by properly manipulating both plungers simultaneously any desired combination of f_A and f_B can be obtained. Mathematically this can be seen as follows: suppose that mode A is a TE mode, and that the values of α and β for $f=f_A$ are given by α_A and β_A. Substituting these values into the characteristic equation obtained by dividing (6a) by (6b), and performing algebraic manipulations, we obtain for mode A

$$\frac{\beta_A}{\alpha_A}\tan\beta_A L\tanh\alpha_A S_2\tanh\alpha_A S_3 - (\tanh\alpha_A S_2+\tanh\alpha_A S_3)=\frac{\alpha_A}{\beta_A}\tan\beta_A L;$$

for mode B, assuming it is also a TE mode, we obtain

$$\frac{\beta_B}{\alpha_B}\tan\beta_B L\tanh\alpha_B S_2\tanh\alpha_B S_3 - (\tanh\alpha_B S_2+\tanh\alpha_B S_3)=\frac{\alpha_B}{\beta_B}\tan\beta_B L.$$

Two equations in the two variables S_2 and S_3 are thus obtained. There will be one value of S_2 and one value of S_3 which will satisfy the above two equations. Any combination of f_A and f_B within the tuning range of the cavity can be obtained by properly positioning the two plungers.

Control over two resonant frequencies could be useful in a number of ways. For example, this cavity could be used in a microwave maser, where resonances are needed at both the signal and pump frequencies. Another possible use of this tuning property would be in making two resonant modes degenerate in frequency, or, conversely, in removing an unwanted degeneracy. Not only can one make frequencies degenerate one can also tune this degenerate frequency.

B. Possible Uses

1) *Solid-State Microwave Masers:* The cavities described in this paper are particularly well suited for use in solid-state microwave masers. Their properties of a) frequency tunability while maintaining large filling factor; b) relatively large unloaded Q's (compared to

other possible dielectric-loaded cavities); and c) simplicity, make them attractive for this application.

Recently there has been interest in optically-pumped microwave masers which amplify at microwave frequencies while being pumped at optical frequencies. In an optically-pumped maser, there must be some opening in the cavity through which the pump light can enter and then travel through the maser material. This opening could be provided by removing the plunger of the single-ended cavity, allowing the light to enter the open end. Or, one of the plungers of the double-ended cavity could be removed to allow passage of the pump light, while the other plunger is used to tune the cavity resonant frequency.

2) *Microwave Paramagnetic Resonance Spectroscopy:* The single- and double-ended cavities may also be useful tools in microwave EPR spectroscopy. Many of the same properties which make these cavities useful for maser applications make them also attractive for spectroscopy.

3) *Microwave Modulation of Light:* Light has been modulated at microwave frequencies through use of the electro-optic effect in various materials. In one modulation technique, a microwave structure containing the electro-optic material is required which a) is resonant at the microwave modulating frequency, and b) will allow passage of the light through the material. A structure that fulfills these requirements is the double-ended cavity with both plungers removed. For this application, the most important cavity properties are electric filling factor and unloaded Q.

4) *Reducing the Size of Microwave Cavities:* It is sometimes desirable or necessary to reduce the size of a microwave cavity by loading it with dielectric material. The single- and double-ended cavities offer a method of accomplishing this while retaining frequency tunability. Through use of the equations and graphs for Q_{WL} and Q_{DL}, one can determine precisely the effect of the dielectric upon the unloaded Q.

5) *Uses of the Cavity Analysis:* The equations of this paper, although derived for the single- and double-ended cavities, are useful also for other situations. In particular, they should be useful for analyzing resonances in waveguide windows. The problem of electrical breakdown in waveguide windows is becoming increasingly important as the power outputs of microwave tubes are pushed higher and higher.

References

[1] E. O. Ammann and R. J. Morris, "Tunable, Dielectric-Loaded Microwave Cavities Capable of High Q and High Filling Factor," Stanford Electronics Laboratories, Stanford, Calif., Rept. No. SEL-63-012 (TR No. 211-4); May, 1963.
[2] R. J. Morris, R. L. Kyhl, and M. W. P. Strandberg, "A tunable maser amplifier with large bandwidth," PROC. IRE, vol. 47, pp. 80–81; January, 1959.
[3] E. T. Jaynes, "Ghost modes in imperfect waveguides," PROC. IRE, vol. 46, pp. 416–418; February, 1958.
[4] M. P. Forrer and E. T. Jaynes, "Resonant Modes in Waveguide Windows," IRE TRANS. ON MICROWAVE THEORY AND TECHNIQUES, vol. MTT-8, pp. 147–150; March, 1960.
[5] M. P. Forrer, "On the Boundary Value Problem of Waveguide Windows," Microwave Laboratory, W. W. Hansen Laboratories of Physics, Stanford, Calif., M. L. Rept. No. 575; March, 1959.
[6] S. Ramo and J.R. Whinnery, "Fields and Waves in Modern Radio," J. Wiley and Sons, Inc., New York, N. Y., pp. 351–353; 1953.
[7] I. G. Wilson, C. W. Schramm, and J. P. Kinzer, "High Q resonant cavities for microwave testing," *Bell Sys. Tech. J.*, vol. 25, pp. 408–434; July, 1946.
[8] Ramo and Whinnery, *op. cit.*, pp. 386–388.
[9] L. C. Maier, Jr. and J. C. Slater, "Field strength measurements in resonant cavities," *J. Appl. Phys.*, vol. 23, pp. 68–77; January, 1952.